An Experimental Approach to Correcting Counting Errors in the Aerodynamic Particle Sizer (APS Model 3310)

Avula Sreenath*, Gurumurthy Ramachandran, James H. Vincent*****

(Received: 15 January 1999; resubmitted: 3 September 1999)

Abstract

This paper describes the different ways of analyzing the output of a real-time device for measuring and counting airborne particles, the aerodynamic particle sizer (APS). This instrument is very widely used in aerosol research throughout the world. It is a time-of-flight instrument in which a particle's measured transit time in the changing flow in a jet passing between two laser beams is converted to its aerodynamic diameter. As the particle passes between the two laser beams, two signal processors, the small particle processor (SPP) and the large particle processor (LPP), independently provide measures of the particle's transit time from the light pulses that are produced. This information is related to the aerodynamic particle diameter of the particle (d_{ae}) by means of calibration against 'unit' density (1000 kg/m^3) spheres. If more than one particle is involved in the analysis of particle transit time, then it gives rise to coincidence effects, resulting in 'phantom' particle generation. The SPP is known to generate phantom counts, while the LPP is known to reduce phantom counts. A new method is described in this paper that gives guidance on how to deal with such coincidence problems. The principle is that it relies on additional information to obtain 'correction factors'. In this case, well-established theory for the aspiration efficiencies of thin-walled aerosol sampling probes has been used along with corresponding experimental data obtained in a wind tunnel using the APS. Results using this method are compared with various other methods that have been tried in the past. The paper provides insights on to how the user can operate the APS to avoid counting errors like those described, and the advantages and limitations of different correction methods are discussed.

1 Introduction

The aerodynamic particle sizer (APS©, TSI Inc., St. Paul, MN) is a direct-reading instrument for counting and measuring the aerodynamic diameters (d_{ae}) of sampled aerosol particles. It is a 'time-of-flight' instrument that detects the velocity of particles relative to the airflow in an accelerating nozzle by determining the particle transit time between two laser beams. As the particle passes through the sensing zone, two light pulses are produced and detected by photodetectors. The resultant electronic pulses trigger a timer and so provide the basis of the measurement of the transit time. By calibration using polystyrene latex (PSL) spheres of known density, the transit time provides a direct measure of d_{ae} (*Wang* and *John* [1]).

The major factors influencing the accuracy of the APS are particle density, particle shape factor, particle deformation and the particle counting process (*Wang* and *John* [1], *Baron* [2], *Ananth* and *Wilson* [3], *Brockmann* et al. [4], *Brockmann* and *Rader* [5], *Chen* et al. [6–8], *Cheng* et al. [9], *Griffiths* et al. [10], *Heitbrink* et al. [11] and *Heitbrink* and *Baron* [12]). The last factor relates to a class of situations in which particle count errors arise from the way in which the particles are detected and timed, and may be both statistical and physical in nature. Despite the widespread use of this version of the APS instrument in aerosol research throughout the world, such errors have previously been addressed by only a few researchers (e.g., *Heitbrink* et al. [11] and *Heitbrink* and *Baron* [12]) and remain poorly understood.

This paper presents a new approach to the development of correction methods. The key ingredient is the application of additional external information to how the raw data from the APS Model 3310 are processed and interpreted. In the case in point, that additional information is provided in the form of what is well-known theoretically about the aspiration efficiencies of certain simple aerosol samplers (i.e., thin-walled probes). This then provides a means by which to correct data, using the APS, obtained from experimental studies of other aerosol samplers.

* Dr. *A. Sreenath*, TSI Incorporated, Shoreview, MN, 55126 (USA).

** Dr. *G. Ramachandran*, (to whom correspondence should be addressed), Assistant Professor, Division of Environmental and Occupational Health, School of Public Health, University of Minnesota, Minneapolis, Box 807 Mayo, 420 Delaware Street, S.E., MN 55455 (USA).

*** Dr. *J. H. Vincent*, Professor and Chair, Department of Environmental and Industrial Health, School of Public Health, University of Michigan, 109 S. Observatory Street, Ann Arbor, MI 48109-2029 (USA).

2 Coincidence Effects

Accurate measurement of d_{ae} for a single particle by the APS Model 3310 requires detection of two light pulses from the same particle. The temporal difference between these two pulses of light is determined by means of two timers, the first referred to as the '*small particle processor*' (SPP) and the second as the '*large particle processor*' (LPP). The SPP is specifically designed to count small particles (that have small transit times) and LPP to

 0934-0866/99/257–265 $17.50+.50/0

count large particles (that have large transit times). The SPP measures particle transit times in 4-ns increments while the LPP measures particle transit times in 66.67-ns increments. The number of particles counted for different transit times are stored electronically in accumulator channels which, as already mentioned, are related to d_{ae} by calibration against standard particles (e.g., polystyrene latex spheres). The operating conditions for SPP and LPP counting have been described and reviewed thoroughly by *Heitbrink* et al. [11].

Heitbrink et al. showed that coincidence can be encountered in three possible ways, as shown in Figure 1. Here, the pulses due to the first particle (A) are given as A_1 and A_2, and those due to the second particle (B) by B_1 and B_2. In **Case 1**, the second pulse of the first particle, A_2, is too small to be detected due to the change in the light scattering efficiency of the particle when the particle is oriented differently to the laser beam or due to non-uniform refractive index or density. As a result, the timer waits for a certain time that defines the largest particle that can be sized. But before the timer is turned off, a second particle arrives at the first laser beam, creating a second pulse. Hence, the first pulse of the first particle (A_1) and the first pulse of the second particle (B_1) are recorded as a transit time for—apparently—a single particle. Hence two real particles are replaced by a single 'phantom' particle.

There are times for both the SPP and LPP during which pulses may not be sensed, despite the presence of a particle in the sensing medium. These are referred to as '*dead times*' and are determined by the counting logic for the timers. In **Case 2**, therefore, the second particle arrives at the first laser beam during the dead-time period of the timer. Now, if A_2 is below the detection threshold and B_2 is detected before the timer switches itself off (i.e., at the end of the maximum transit time), a 'phantom' particle is again created that replaces the two real particles. For both Cases 1 and 2, the resultant apparent particles are referred to as '*open-timer phantom*' particles. This is because the timer of the instrument creates these particles during a condition where the timer remains 'open' (that is when the timer is counting). This condition can be caused not merely by increased particle concentration at the inlet of the APS but also due to a variety of other reasons. These include changes in particle orientation to the laser beam (resulting in varying light scattering intensity produced by the same particle), very long transit time by a particle, or a large concentration of small particles that do not produce one or more pulses above the detection threshold (*Heitbrink* et al. [11]). Hence, open-timer phantom counts are created only when a large number of single pules are created by particles. With this random addition of phantom particles for the SPP, the background concentration is known to increase with increasing particle size (*Gudmundsson* and *Lidén* [13]).

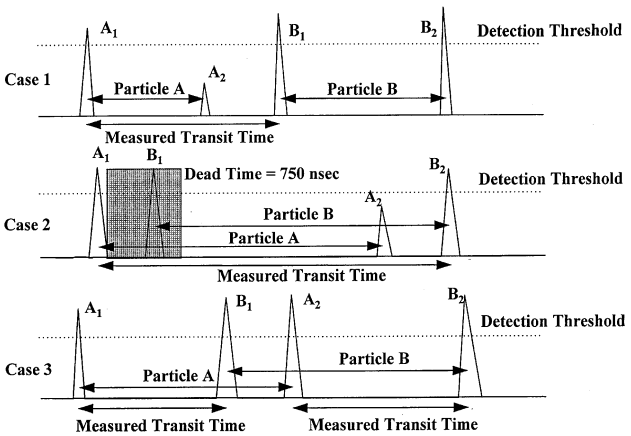

Fig. 1: Schematic of the analogue output of the SPP showing the three possible combinations for phantom particle generation in the APS.

In **Case 3**, 'phantom' particle generation occurs when B_1 is generated before A_2. The net result here is the apparent generation of two phantom particles from a single actual particle. This is often referred to as an '*overlap phantom*' particle. To combat this, *Heitbrink* and *Baron* [12] recommended reduction of small diameter particle concentration (to not more than 100 particles/cm^3) as a possible remedy.

Of the two processors in the APS circuitry, the SPP tends to create 'phantom' particles along the lines indicated above, while the LPP is designed to prevent creation of phantom particles and has a lower effective counting efficiency. The overall effective range of particle aerodynamic diameter for the APS is from about 0.5 µm to 30.5 µm. In the practical use of the APS Model 3310, for d_{ae} less than 5.42 µm, the SPP accumulator channels alone are used; but for d_{ae} from 16.0 µm to 30.5 µm, the LPP accumulator channels alone are used. In the overlap region of d_{ae} between 5A2 and 14.9 µm, information from both the SPP and LPP is used, and this is where the problems occur. In one correction procedure recommended by the manufacturer of the APS, the weightings for the SPP counts are gradually and linearly decreased and the weightings for the LPP counts are correspondingly increased (as described in the TSI Advanced Software Manual, 1988).

Before going into the details of the analysis of APS output files, it is necessary to describe the way in which APS stores data. The APS stores particle count data for individual particle sizes from channels 0 to 78. (Note: Here, the '*channels*' are different from what are earlier referred to as '*accumulator channels*'). Channels 0 to 50 correspond to the SPP which has the 4-ns timer. Channels 51 to 62 correspond to data from the LPP which has the 66.67-ns timer. Channels 63 to 78 also represent LPP data, but in the overlap region that corresponds to channels 36 to 50 of the SPP data. Hence, channels 63 and 36 correspond to the same particle diameter, channels 64 and 37 correspond to the same particle diameter, and so on.

3 Previous Efforts to Minimize Coincidence

Two broad approaches can be taken to minimizing coincidence effects. The first involves reducing the actual counts by physically adjusting the photomultiplier (PMT) output. Reducing phantom particle counts may be achieved by adjusting the LPP to extend its range to particle sizes below 5 µm (*Gudmundsson* and *Lidén* [13]). In this approach, only the LPP data are used and the SPP data are discarded. There are two PMT adjustments, one is the PMT gain and the other is the amplifier gain. The former changes both the PMT dc background level and the amplitude, while the latter changes only the amplitude. However, it is noted that the PMT gain should not be reduced too much since it may result in a dramatic reduction in counting efficiency for certain particle sizes which will in turn skew the actual particle size distribution.

The second approach involves making numerical adjustments to the counts after they have been recorded. Here it should be noted that, while the SPP contains phantom particles and hence overestimates particle counts, the LPP underestimates the counts for

small-diameter particles in the overlap region. In a particle size distribution dominated by phantom particle counts, the degree of under-estimation by the LPP is not as severe as the degree of over-estimation by the SPP. Hence, looking at the counts of the diameters of common channels, it is, in principle, possible to predict the phantom counts, and eventually to subtract the phantom counts from the corresponding SPP channels in the overlap region (*Heitbrink* and *Baron* [12]). This approach has been tested in relation to the current study and will be discussed later.
Mathematically, there are 4 different ways (*Maynard* [14]) in which the phantom counts may be removed from the raw data file, as follows:

1. An average is taken of the difference between the SPP (which has more counts than the LPP) and the LPP, and this is subtracted from the SPP for all channels in the overlap region;
2. Instead of an average of the difference between SPP and LPP as in Step 1, a linear fit is made to the difference in counts between the SPP and the LPP. This equation as a function of aerodynamic diameter is used to deduce counts from the SPP in the overlap region;
3. Similar to Step 2 except that instead of linear fit, a polynomial fit is used to represent the difference in counts;
4. As described in the TSI Advanced Software Manual, a series of correction factors or 'extrapolation factors' is recommended to be used on the counts in the SPP and LPP channels in the overlap region in such a way that there is progressively increasing weight given to the LPP data (and so progressively decreasing weight given to the SPP data).

The major drawback in all the above methods is the assumption that the LPP counts are true counts in the entire overlap range (*i.e.*, d_{ae} from 5.42 to 14.9 μm). However, this is not the case due to the fact that the LPP underestimates particle counts for small particles (since they are not fully detected). As a result, therefore, the difference between the SPP and LPP counts for particles in the overlap size range my be greater than predicted.
The correction factors recommended by TSI are shown in Table 1. These were derived purely on the basis of statistical analysis of the probability of phantom counts occurring in the SPP in the overlap region. However, to our knowledge, these correction factors have never been validated experimentally. Indeed, the APS software supplied with the instrument does not provide any routine for merging the SPP and LPP data, nor does the accompanying literature warn the user about phantom counts.
Heitbrink et al. [11] performed an experiment using aluminum oxide aerosol at a concentration of 120 particles/cm^3 and with 90% of all particles less than 15 μm. From their results, they developed a statistical method to predict the count of single pulses and so to estimate the concentration of open-timer phantom particles. However, this method itself my sill carry a considerable amount of statistical uncertainty in the corrected data. Further, there is no way to determine whether the correction made to the particle counts in this way is adequate.

Table 1: Table of correction factors used by TSI.

Particle aerodynamic diameter (μm)	SPP Channel #	SPP Correction Factor	LPP Channel #	LPP Correction Factor
5.42	36	15/16	63	1/16
5.83	37	14/16	64	2/16
6.26	38	13/16	65	3/16
6.73	39	12/16	66	4/16
7.23	40	11/16	67	5/16
7.77	41	10/16	68	6/16
8.35	42	19/16	69	7/16
8.98	43	8/16	70	8/16
9.65	44	7/16	71	9/16
10.4	45	6/16	72	10/16
11.1	46	5/16	73	11/16
12	47	4/16	74	12/16
12.9	48	3/16	75	13/16
13.8	49	2/16	76	14/16
14.9	50	1/16	77	15/16

5 The New Approach to Minimizing Counting Errors

In our new approach, we adjusted the SPP and LPP counts by reference to measured particle counts in an experiment where we had separate—and reliable—physical knowledge. The key ingredient, therefore, is the introduction of this additional information. In general, that information should come from some other knowledge (e.g., theoretical) about the physical system in which the APS is being used. For the specific case reported here, that additional information comes from our theoretical knowledge of the aerosol sampling system that was being studied experimentally with the APS. Experiments were conducted in which we used the APS Model 3310 to determine the aspiration efficiency of a thin-walled sampling probe in a wind tunnel. We then adjusted particle counts to make the results match what was known from classical aerosol sampling theory. Here we took advantage of the fact that thin-walled probes have been extensively studied by aerosol scientists for several decades, and that well-proven theories exist for predicting their aspiration efficiencies both facing the freestream and for angles (α) up to 90° to the freestream (*Vincent* [15]). In the present paper, the approach taken was to focus on the particular condition, $\alpha = 90°$.

5.1 Experimental

5.1.1 Apparatus and Experimental Procedures

The experimental set-up consisted of a small wind tunnel (Figure 2) that has been described in detail elsewhere by *Ramachandran* et al. [16]. The basic experimental procedures were also identical to that described in that paper. The only significant difference is that the primary sampler used here is a thin-walled, cylindrical probe. Therefore, only a brief summary is given here. The wind tunnel test section had a cross-sectional area of

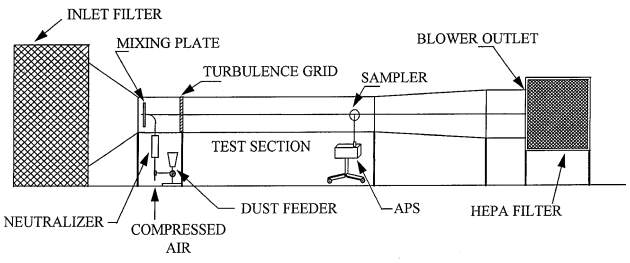

Fig. 2: Schematic of the wind tunnel used in the experiments.

$0.3\,\mathrm{m} \times 0.3\,\mathrm{m}$ in which the windspeeds could be varied in the range from $0.25\,\mathrm{ms}^{-1}$ to $25\,\mathrm{ms}^{-1}$. Polydisperse glass beads in the size range from about 1 to 50 µm were injected ahead of the working section using an NBS mechanical dust feeder (BGI Inc., Waltham, MA), providing a uniform spatial and temporal distribution of aerosol concentration.

The thin-walled sampling probe system was arranged as shown schematically in Figure 3. In this system, particles were aspirated at a sampling flowrate of 5 liters min^{-1} (i.e., the APS sampling flowrate) into a thin-walled tube of outer diameter 1 cm which tapered to 0.6 cm at its inlet. The tube was able to rotate about the vertical axis so that the orientation of the entry with respect to the freestream (α) could be arranged as desired. In the experiments described below, all sampler surfaces near the entry were greased in order to prevent errors associated with particle bounce and/or rebound. Furthermore, the test sampler was electrically grounded to minimize possible errors associated with electrostatic charge effects.

In our experiments, we set out to determine the ratio of the particle counts recorded by the APS when the sampler inlet was oriented at $\alpha = 90^\circ$ ($_{APS}c_{\alpha=90}$) to that when the sampler was facing forward ($_{APS}c_{\alpha=0}$). We will call this ratio $H_{\alpha=90}$ where,

$$H_{\alpha=90} = \frac{{}_1c_{\alpha=90}}{{}_1c_{\alpha=0}}. \tag{1}$$

For each measurement of $H_{\alpha=90}$, the number concentration was measured eleven times: six times at the forwards-facing orientation to provide an average value of $_{APS}c_{\alpha=0}$, and five times at orientation α to provide an average value of $_{APS}c_{\alpha=90}$. To ensure that any count differences between the positions were not caused by systematic temporal shifts in the aerosol generation rate, the concentrations were measured at the two positions in a '0-α-0-α-0-α-0-α-0-α-0' sequence. In reality, the aerosol concentration in the wind tunnel was able to be maintained constant to within about 1% over periods of at least 1 hour. For all the experiments performed in the wind tunnel, the free stream velocity (U_0) was set at 4.0 m/s. The sampling flow rate was set at 5 lpm (sampling flow rate of the APS) which corresponds to an inlet velocity (U_s) of 2.63 m/s for the thin-walled probe. Hence, the velocity ratio ($R = U_0/U_S$) was fixed at 1.52 for all experiments in the wind tunnel.

Some additional validation experiments were carried out towards the end of the project in which the thin-walled probe was replaced by a 6.35 cm-diameter spherical blunt sampler with a 6.35 mm-diameter circular orifice (as described below). This is the same sampler that was the subject of other work from our group reported elsewhere (*Ramachandran* et al. [16]).

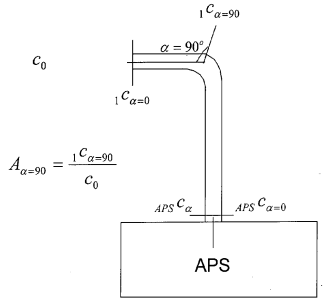

Fig. 3: Schematic of the thin-walled probe sampling system.

5.1.2 What was measured?

As already stated, the aim of the experiments was to make measurements that could ultimately be related to the aspiration efficiency of the thin-walled probe oriented at 90° to the freestream ($A_{\alpha=90}$). Here, by '*aspiration efficiency*', we refer to the ratio of the particle concentration passing through the plane of the sampler entry (i.e., the entrance to the tube) to that in the undisturbed freestream concentration. In the science of aerosol sampling, this has come to be regarded as the most fundamental metric of sampler performance, relating purely to aerodynamic processes by which particles are conveyed into the sampler from the outside environment (*Vincent* [15]). In our experiments, what was actually measured was the ratio $H_{\alpha=90}$, as defined above. We now need to consider how this relates to aspiration efficiency.

Figure 3 is a schematic diagram of the sampling system and provides the basis for making this link. Here we may define '*sampling efficiency*' (as opposed to aspiration efficiency itself) as

$$E_\alpha = \frac{_{APS}c_\alpha}{c_0} \tag{2}$$

where $_{APS}c_\alpha$ is the particle concentration reaching the APS for the general orientation α. In contrast to aspiration efficiency, this inevitably also incorporates the particle losses that take place as the air is transported from the sampler entry all the way down to the sensing zone of the APS. It is related to $H_{\alpha=90}$ for the particular case of interest (i.e., $\alpha = 90^\circ$) by the expression way

$$H_{\alpha=90} = \frac{_{APS}c_{\alpha=90}}{_{APS}c_{\alpha=0}} = \frac{E_{\alpha=90}}{E_{\alpha=0}}. \tag{3}$$

Since the orientation of the tube with respect to the vertical remained fixed during the experiments, regardless of the orientation of the inlet with respect to the freestream, gravity effects were constant. So particle losses by deposition over the majority of the length of the tube could be assumed constant between the two conditions $\alpha = 90^\circ$ and $\alpha = 0^\circ$. Although for arbitrary orientation of the entry there would be orientation-dependent losses of particles to the inside wall dose to the sampling inlet (by impaction), such losses would not be present for $\alpha = 90^\circ$ because the inside wall of the tube projects zero area to the incoming air flow. So for $\alpha = 90^\circ$, it is reasonable to assume that particle losses along the whole length of the tube would be the same for both orientations. With this in mind, therefore, $H_{\alpha=90}$ reverts to the simpler form of Eq. (1)

$$H_{\alpha=90} = \frac{{}_1c_{\alpha=90}}{{}_1c_{\alpha=0}} \tag{4}$$

where the subscript '1' refers to the concentration at the entrance to the thin-walled sampler. Since aspiration efficiency is written as

$$A = \frac{{}_1c_\alpha}{c_0}. \tag{5}$$

Eq. (3) becomes

$$H_{\alpha=90} = \frac{A_{\alpha=90}}{A_{\alpha=0}} \tag{6}$$

or, more to the point,

$$A_{\alpha=90} = H_{\alpha=90} \cdot A_{\alpha=0}. \tag{7}$$

From our experiments, measured values of $A_{\alpha=90}$ (from the measured values of $H_{\alpha=90}$ and calculated $A_{\alpha=0}$), can be directly compared with corresponding values of $A_{\alpha=90}$ derived from theory. The object of the exercise, then, is to correct the APS

particle counts contributing to $H_{\alpha=90}$ in order to bring experiment and theory into agreement.

5.2 Results and Discussion

Figure 4 compares aspiration efficiency, $A_{\alpha=90}$, obtained experimentally with that calculated from theory (*Vincent* et al. [18]; *Hangal* and *Willeke* [20]). It shows separately the results obtained using counts from both the SPP and the LPP. It also shows that both theoretical models predict a fall in $A_{\alpha=90}$ with increasing particle diameter, d_{ae}. This trend is not reflected in the uncorrected experimental $A_{\alpha=90}$ results. When comparing the combined SPP and LPP data, $A_{\alpha=90}$ is seen to increase in the range d_{ae} from about 5.0 to 15 µm, followed by a sharp drop beyond 15 µm. The first part of this observed trend is physically unrealistic unless particles are being added externally in some way during sampling. But such addition would be possible due only to particle bounce or reentrainment effects, and—as mentioned earlier—the sampler surfaces were thoroughly greased to reduce such effects. Hence, the observed increase in $A_{\alpha=90}$ can only be attributed to spurious counts in the SPP. These appear to increase with increasing particle size beyond 5 µm. Further, such spurious counts also introduce a discontinuity during the switch from the SPP to the LPP; that is, beyond $d_{ae} = 14.9$ µm. Although it may seem logical to assume that coincidence effects too would cancel out (since aspiration efficiency in this set of experiments is determined by taking the ratio of two concentration measurements), this was not the case because the phantom counts depended on the aerosol concentration being sampled. It is a fact that, for $\alpha = 90^\circ$, very few particles were sampled compared to $\alpha = 0^\circ$.

In order to merge the SPP and LPP data, we first considered the TSI algorithm given in the APS Advanced Software Manual (see Table 1). Figure 5 clearly illustrates the effect of using this correction, and we see that the new $A_{\alpha=90}$ values thus generated appear to be somewhat more realistic in relation to theory. However, it is clear that the corrections that have been applied are not really adequate since the deviation from theory still persists and the physically unrealistic phenomenon of the apparent 'addition' of particles still persists. TSI correction factors are linear, a way to gradually increase the contributions of LPP and reduce contributions by SPP in the overlap zone (SPP and LPP correction factors must always add up to one for any particle size in the overlap zone). This method of interpolation also assumes that the efficiency curves for the SPP and LPP are also monotonic, in the sense that the SPP efficiency steadily increases (due to phantom counts) while the LPP efficiency increases (again depending on the APS gain) with increasing particle diameter. The TSI correction factors are thus meant to compensate for these inefficiencies by suppressing the SPP counts and boosting the LPP counts to predict the actual concentration.

The SPP and LPP efficiencies depend on a number of factors. The photomultiplier tube (PMT) voltage and gain play a major role in influencing the efficiencies of the processors. But the APS does not have individual controls for the SPP and LPP gains, the overall gain has to be adjusted for both processors simultaneously. Since it is obvious that the SPP requires a low gain and the LPP requires a high gain, the user must look for an optimum value. Having a low gain is usually preferred since the low gain will help the APS to avoid counting too many small-diameter particles that are a major source of phantom counts. But, at the same time, the LPP counting efficiencies may be too low for small-diameter particles (5 to 15 µm). Having a high gain will result in the SPP becoming too sensitive, thereby skewing the measured size distribution and also increasing phantom particle counts. Another approach to reducing phantom counts and thus increasing the reliability of the SPP is to use the APS only at low particle concentration. But for experiments where the entire range of the APS is crucial, reducing the concentration of the aerosol sampled by the APS will increase Poisson errors, especially for large-diameter particles which are difficult to transport through the sampling system and the inlet of the APS.

In the method suggested by *Heitbrink* and *Baron* [12], the difference in counts between the SPP and the LPP in the overlap

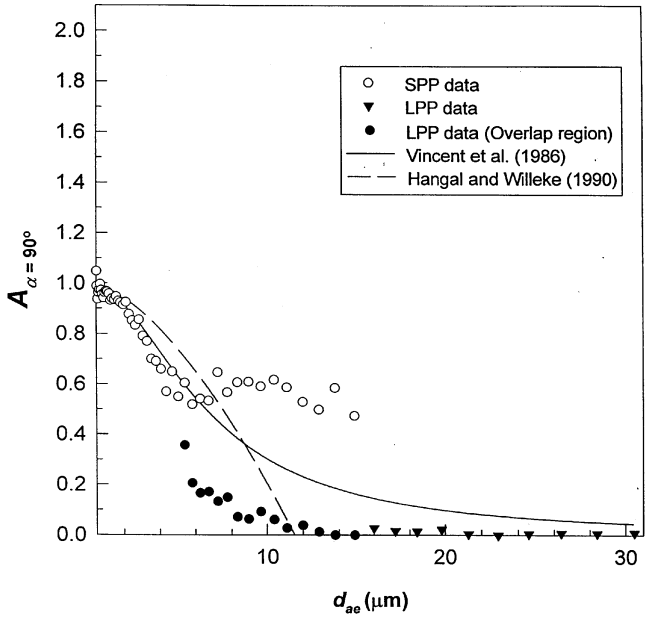

Fig. 4: Plot of aspiration efficiency ($A_{\alpha=90}$) as a function of particle aerodynamic diameter (d_{ae}) for the thin-walled probe at $\alpha = 90^\circ$, comparison between experiment and theory.

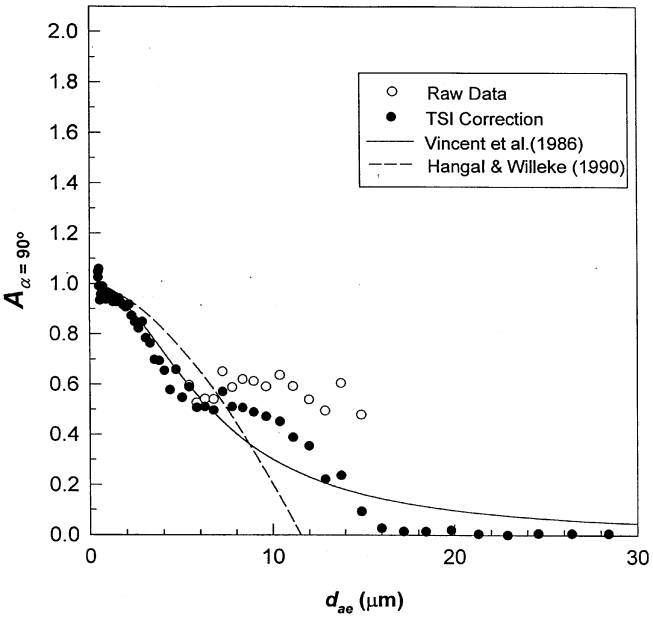

Fig. 5: Plot of aspiration efficiency ($A_{\alpha=90}$) as a function of particle aerodynamic diameter (d_{ae}) for the thin-walled probe at $\alpha = 90^\circ$, application of the TSI correction factors.

region is used as a basis to estimate phantom counts. In the approach suggested by *Maynard* [14], the difference between the SPP and the LPP in the overlap region was used to determine either an average phantom count or to develop a function (by curve fitting) that defines the phantom counts with respect to particle aerodynamic diameter. Here, a linear or quadratic form for this function should be adequate. This function, or a mean phantom count, is then subtracted from all the SPP channels, thereby minimizing the effect of phantom counts. The corrected SPP data are then blended with the LPP data using the TSI correction factors for the overlap region (see Table 1 for the tabulation of correction factors). This approach is adopted for both the reference concentration and the condition for which the aspiration efficiency needs to be determined. Figure 6 compares the different methods of reducing phantom counts and their consequent effect on the measured aspiration efficiency. It is evident from the graph that all these methods tend to over-estimate the coincidence effects, as a result of which the measured $A_{\alpha=90}$ falls much more sharply than predicted theoretically.

5.3 Proposed New Correction Method

It is clear from the above that the particle count correction methods previously examined are not really adequate. As already suggested, a better approach would be to develop correction factors for the APS data with respect to a known physical outcome; for instance, the aspiration efficiency of a thin-walled probe for which theory is well established.

The proposed new approach involves comparing the APS raw data for a thin-walled probe oriented at 90° to the freestream with a theory (*Vincent* and co-workers [15, 17, 18]) that has been well tested. The raw data and the corrected APS data using new correction factors are shown in Figure 7. Here, the new correction factors, shown in Table 2, were developed by matching the raw APS data with theory. The new correction factors were then tested by correcting the approach for a different aerosol sampling situation. An example, this time for the blunt spherical sampler oriented at $\alpha = 180°$, is shown in Figure 8, and it is seen that a good match is obtained. In addition, it is interesting to note that the error bars are also significantly reduced.

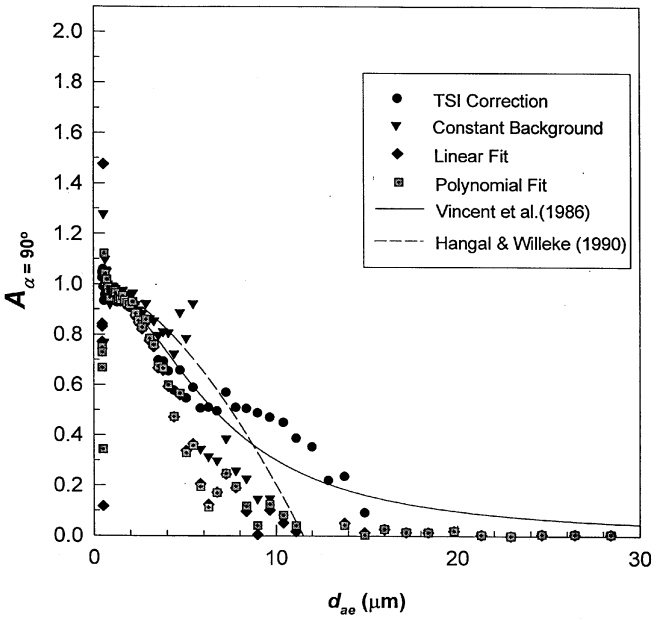

Fig. 6: Plot of aspiration efficiency ($A_{\alpha=90}$) as a function of particle aerodynamic diameter (d_{ae}) for the thin-walled probe at $\alpha = 90°$, comparison of different correction factors.

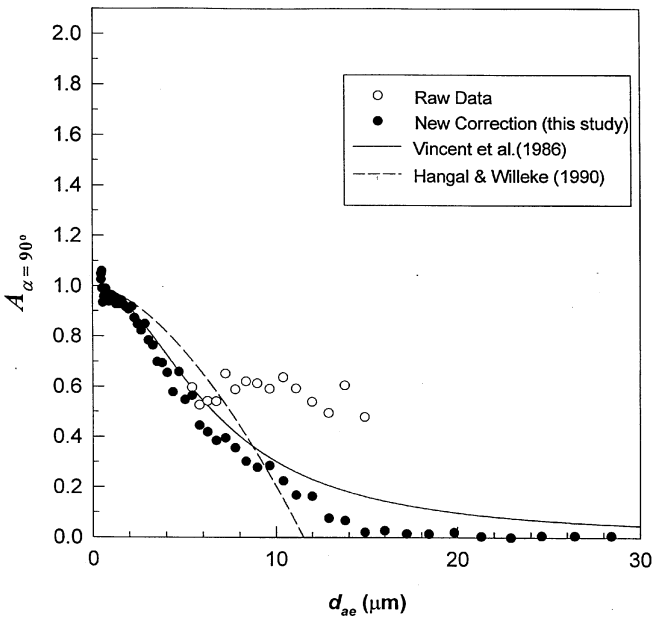

Fig. 7: Plot of aspiration efficiency ($A_{\alpha=90}$) as a function of particle aerodynamic diameter (d_{ae}) for the thin-walled probe at $\alpha = 90°$, comparison between experiment and theory for our new correction factors.

5.4 Wider Implications

The question that arises is: are these correction factors universal for all APS units, particle size distribution and for all sampling conditions. Based on what was already known, the starting hypothesis has to be that they are **not** universal. In order to test this hypothesis, the APS was exposed to two contrasting aerosols: the first the glass beads generated in the wind tunnel, and the second the ambient aerosol present in the laboratory air. The changes produced in the particle size distribution by using the

Table 2: Table of correction factors used in our new approach.

Particle aerodynamic diameter	SPP Channel #	SPP Correction	LPP Channel #	LPP Correction
5.42	36	15/32	63	1/6
5.83	37	14/32	64	2/6
6.26	38	13/32	65	3/6
6.73	39	12/32	66	4/6
7.23	40	11/32	67	5/6
7.77	41	10/32	68	6/6
8.35	42	19/32	69	7/6
8.98	43	8/32	70	8/6
9.65	44	7/32	71	9/6
10.4	45	6/32	72	10/6
11.1	46	5/32	73	11/6
12	47	4/32	74	12/6
12.9	48	3/32	75	13/6
13.8	49	2/32	76	14/6
14.9	50	1/32	77	15/6

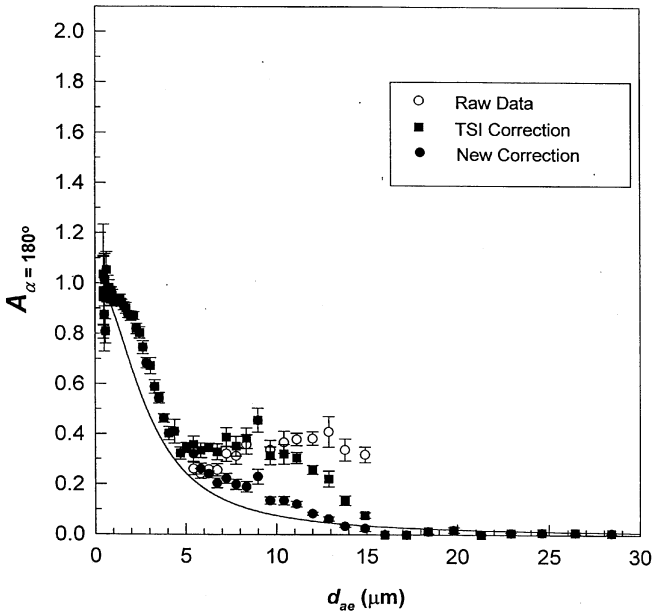

Fig. 8: Plot of aspiration efficiency ($A_{\alpha=90}$) as a function of particle aerodynamic diameter (d_{ae}) for the spherical blunt sampler at $\alpha = 90^\circ$, comparison between experiment and theory for our new correction factors.

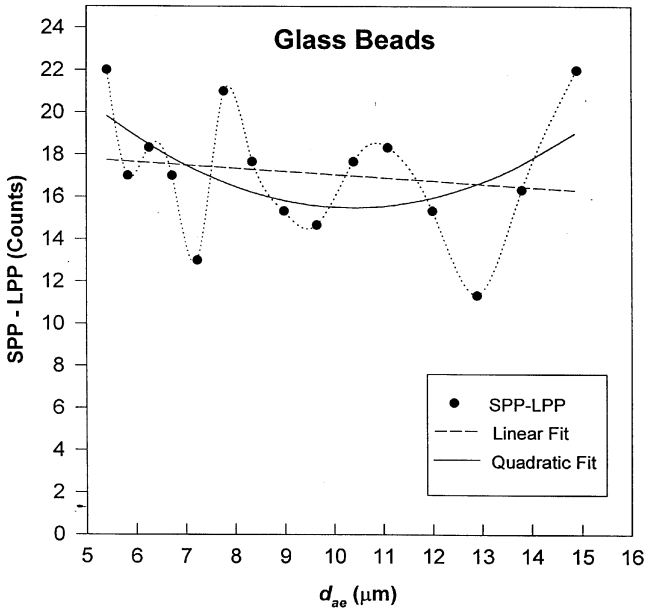

Fig. 10: Plot of the difference in counts between the SPP and LPP in the overlap region for the glass bead test aerosol.

different correction methods—including the new one proposed in this paper—were compared. The results shown in Figure 9 for the glass beads reflect the frequency distribution of those particles counted by the APS for the different correction methods. It is evident that the differences are not very significant. As mentioned earlier, the difference between the SPP and LPP counts in the overlap region gives a measure of phantom counts. As shown in Figure 10, it is clear that this difference is fairly constant over the whole region. In turn, therefore, any differences between the correction methods would not produce a significant effect in the measured particle size distribution. By contrast, consider the same problem for the frequency distribution as determined using the APS for the ambient aerosol (Figure 11). Now, unlike for the glass beads, there are clear differences in the particle size distributions obtained using various correction methods. While most of the correction methods underestimate the counts compared to the raw data, the new correction method actually overestimates the counts especially in the overlap region. It also produces a discontinuity in the frequency distribution during the switch from SPP-only to the overlap region. Figure 12 shows a plot of the difference in the SPP and LPP counts in the overlap region. In contrast to what was seen in Figure 10 for the glass beads, here it is evident that the differences between the SPP and LPP counts in the overlap region decreased with increasing d_{ae}. Phantom particles were also significantly higher than for the earlier case of glass beads in wind tunnel. The larger the difference between the SPP and LPP counts, the more the phantom particle generation. A linear or a quadratic fit to the difference in counts between SPP and LPP is obtained first as a function of d_{ae} and this function is used to subtract from the total counts the estimated phantom count using that function from all the channels. Consequently, more is subtracted from channels corresponding to small particle diameters than from

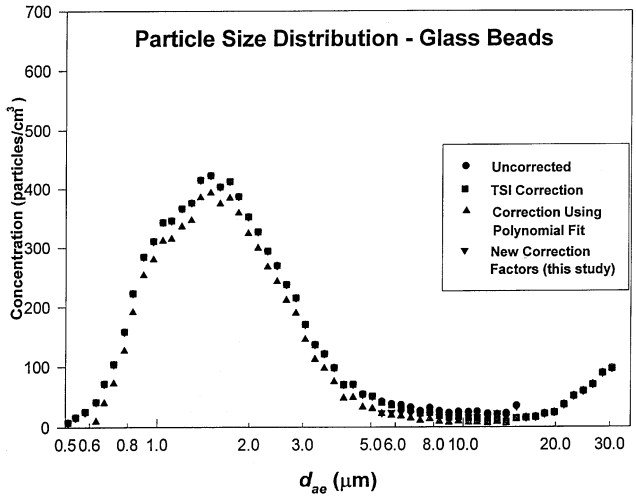

Fig. 9: Plot of the particle frequency size distribution for test aerosol (glass beads) used in the wind tunnel.

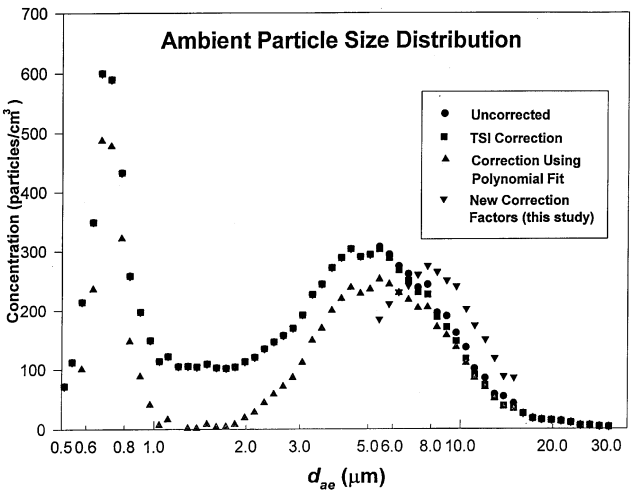

Fig. 11: Plot of the particle frequency size distribution for ambient aerosol in our laboratory.

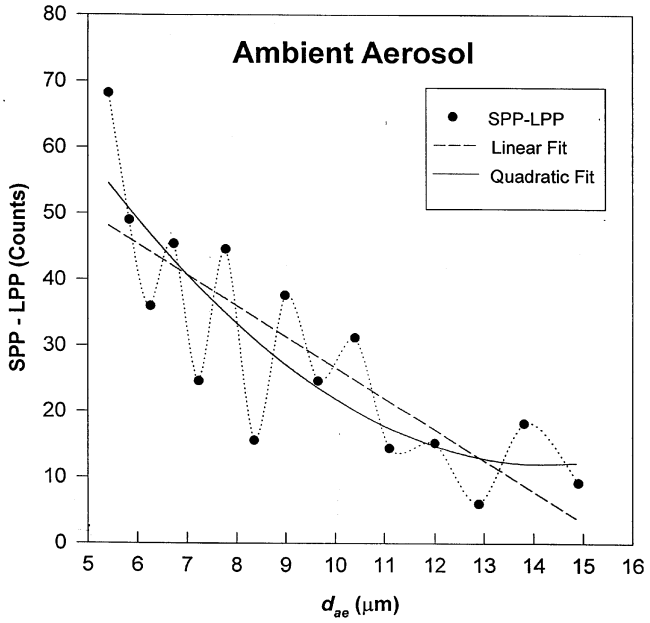

Fig. 12: Plot of the difference in counts between the SPP and LPP in the overlap region for the ambient aerosol.

those for the larger diameters due to the nature of this function. Use of polynomial methods results in reduction of all the SPP counts, even for particle diameters less than 5 μm, a range where the SPP is known to be efficient and therefore needing no correction.

The new approach for correcting the APS counts modifies data only in the overlap region. It adopts the TSI counting logic for particles less than 5 μm, where no corrections to the raw data are made. While this is preferable, it does lead to certain other problems; for example, the observed discontinuity in the corrected counts in the overlap region. This again points to the fact that the APS correction factors to be used are dependent on the size distribution of the aerosol being sampled.

The discontinuities arise because the new correction factors do not converge towards 1 (unlike the TSI correction factors that do). However, such convergence is not actually required. The correction factors are dependent on the size distribution of the aerosol (mass median aerodynamic diameter and geometric standard deviation) and the PMT settings of the APS in question. The discontinuity is less obvious in Figure 9 than in Figure 11 because the aerosol used was different. It clearly demonstrates that the correction factors proposed in Table 2 are specific to the glass beads used in our experiments. For ambient aerosol, the values in Table 2 cannot be used. Unlike TSI correction factors which are supposedly universally applicable (and hence leading to significant errors under certain sampling situations), our proposed correction factors are specific to the APS and the aerosol used. Our experiments have shown that the TSI correction factors can be inadequate under certain conditions, and that users of the APS need to develop their own correction factors relevant to the specific APS application they have in mind.

Thus it is very important to stress that any recommendation to users of the APS Model 3310 must be highly dependent on the intended use of the APS data. For applications where the ratio of two concentrations is needed, it is advisable to obtain correction factors based on some known result or theory, such as—in our case—the aspiration efficiency of thin-walled probes at 90°. Such a new approach may be used in a laboratory setting where measuring sampling efficiency of different samplers may be of interest. However it is unreasonable to expect all APS users to measure the aspiration efficiency of thin-walled probes in order to develop their own correction factors for their own aerosol situations. The differences between the SPP and LPP counts in the overlap region (5 to 15 μm) should give the user a useful first estimate of the order of magnitude of coincidence error for their sampling conditions. If the difference between the SPP and LPP counts is small and the intention is to determine the particle size distribution and particle size statistics such as count median diameter, mass median diameter and geometric standard deviation, no correction is required. But if the difference between the SPP and LPP counts is large, the user should try to reduce the inlet concentration of the challenge aerosol. The user may also have to lower the PMT gain of the APS in order to avoid counting too many small-diameter particles that may flood the sensing chamber. However, the user needs to exercise caution in lowering the PMT gain especially when there is a need to count small particles accurately. For the experiments discussed in this paper, the interest is more towards counting large particles accurately since for small particles, the sampling efficiency is close to unity. In cases where the user cannot realistically control the inlet concentration below 100 particles/cm^3, it is strongly recommended that the user should use a quadratic fit to the difference between the SPP and LPP counts in the overlap region as a measure of coincidence. This may then be used to subtract particle counts from SPP channels in the overlap region only. Further, it should be noted that the user will need to adopt this procedure **even** if the aerosol concentration is below 100 particles/cm^3 for a highly-polydisperse aerosol with a large geometric standard deviation.

6 Conclusions

It is evident from the above that the APS Model 3310 is a very sensitive and useful instrument. But the data it provides need to be interpreted with great caution. The present work has re-affirmed that the APS is sensitive to the particle size distribution of the aerosol and particle concentration. Other researchers have also shown that APS is sensitive to particle density and the particle shape factor (*Chen* et al. [8, 9] and *Griffiths* et al. [10]). In addition, phantom particle generation is a significant phenomenon and is dependent on the PMT voltage and gain, making it very instrument-specific as well. Hence, simply calibrating the APS is not the only thing the user needs to be concerned about. Ideally, the user should actually verify the output from the APS using a known aerosol particle size distribution, or devise ways to characterize the error in order to come up with suitable correction factors that are appropriate to their application. In this regard, therefore, an innovative approach to correcting and characterizing APS data has been described here.

7 Acknowledgement

This work was carried out under CDC-NIOSH Contract 5 RO1OH02984-03. The authors are grateful for this support.

8 Symbols and Abbreviations

d_{ae} aerodynamic diameter
SPP small particle processor
LPP large particle processor
PMT photo-multiplier tube
dc direct current
α angle made by sampler with the wind direction
${}_{APS}c_{\alpha}$ concentration measured by the APS when the sampler is oriented at angle α
${}_{1}c_{\alpha}$ concentration at inlet of the thin walled sampler
H_{α} c_{α}/c_0, ratio of concentration when sampler is at orientation α to concentration when sampler is at orientation 0°
U_0 free stream velocity
U_s inlet velocity
R velocity ratio $= U_0/U_s$
E_{α} sampling efficiency at angle α, ${}_{APS}c_{\alpha}/c_0$
A_{α} aspiration efficiency, ratio of concentration measured at inlet of sampler at angle α to that measured at angle 0°, ${}_{1}c_{\alpha}/c_0$.

9 References

[1] *H. Wang, W. John:* Particle Density correction for the aerodynamic particle sizer. Aerosol. Sci. Technol. *6* (1987) 191–198.
[2] *P. A. Baron:* Calibration and use of the APS (APS 3300). Aerosol Sci. Technol. *5* (1986) 55–69.
[3] *G. Ananth, J. C. Wilson:* theoretical analysis of the performance of the TSI aerodynamic particle sizer: the effect of density on response. Aerosol Sci. Technol. *9* (1988) 189–201.
[4] *J. E. Brockmann, N. Yamano, D. Lucero:* Calibration of the aerodynamic particle sizer 3310 (APS 3310) with polystyrene latex monodispersed spheres and oleic acid monodispersed particles. Aerosol Sci. Technol. *8* (1988) 279–281.
[5] *J. E. Brockmann, D. J. Rader:* APS response to non-spherical particles and experimental determination of dynamic shape factor. Aerosol Sci. Technol. *13* (1990) 162–172.
[6] *B. T. Chen, Y. S. Cheng, H. C. Yeh:* Performance of a TSI aerodynamic particle sizer. Aerosol Sci. Technol. *4* (1985) 89–97.
[7] *B. T. Chen, D. J. Crow:* Use of an aerodynamic particle sizer as a real-time monitor in generation of ideal solid aerosols. J. Aerosol Sci. *17* (1986) 963–972.
[8] *B. T. Chen, Y. S. Cheng, H. C. Yeh:* An experimental approach to studying particle density effects in the TSI aerodynamic particle sizer (3300). J. Aerosol Sci. *20* (1989) 1489–1492.
[9] *Y. S. Cheng, B. T. Chen, H. C. Yeh:* Behavior of isometric non-spherical aerosol particles in the aerodynamic particle sizer. J. Aerosol Sci. *21* (1990) 701–710.
[10] *W. D. Griffiths, S. Patrick, A. P. Rood:* An aerodynamic particle size analyzer tested with spheres, compact particles and fibers having a common settling rate under gravity. J. Aerosol Sci. *15* (1984) 491–502.
[11] *W. A. Heitbrink, P. A. Baron, K. Willeke:* Coincidence in time-of-flight aerosol spectrometers: phantom particle creation. Aerosol Sci. Technol. *14* (1991) 112–126.
[12] *W. A. Heitbrink, P. A. Baron:* An approach to evaluating and correcting aerodynamic particle sizer measurements for phantom particle count creation. Am. Ind. Hyg. Ass. J. *53* (1992) 427–431.
[13] *A. Gudmundsson, G. Lidén:* Determination of cyclone model variability using a time-of-flight instrument. Aerosol Sci. Technol. *28* (1998) 197–214.
[14] *A. D. Maynard:* Personal communication (1997).
[15] *J. H. Vincent:* Aerosol Sampling: Science and Practice. Wiley, London 1989.
[16] *G. Ramachandran, A. Sreenath, J. H. Vincent:* Towards a new method for experimental determination of aerosol sampler aspiration efficiency in small wind tunnels. J. Aerosol Sci. *29* (1998) 000 pages.
[17] *J. H. Vincent:* Recent advances in aspiration theory for thin-walled and blunt aerosol sampling probes. J. Aerosol Sci. *18* (1987) 487–498.
[18] *J. H. Vincent, D. C. Stevens, D. Mark, M. Marshall, T. A. Smith:* On the aspiration characteristics of large-diameter, thin-walled aerosol sampling probes at yaw orientation with respect to the wind. J. Aerosol Sci. *17* (1986) 211–224.
[19] *K. Okazaki, K. Willeke:* Transmission and deposition behavior of aerosols in sampling inlets. Aerosol. Sci. Technol. *7* (1987) 275–283.
[20] *S. Hangal, K. Willeke:* Overall efficiency of tubular inlets sampling at 0–90 degrees from horizontal air flows. Atmos. Eviron. *24A* (1990) 2379–2386.